

Redox Potential and Equilibria in the Reductive Half-Reaction of *Vibrio harveyi* NADPH–FMN Oxidoreductase[†]

Benfang Lei,[‡] He Wang,[§] Yimin Yu,^{||} and Shiao-Chun Tu*

Department of Biology and Biochemistry, University of Houston, Houston, Texas 77204-5001

Received September 22, 2004; Revised Manuscript Received October 22, 2004

ABSTRACT: *Vibrio harveyi* NADPH:FMN oxidoreductase P (FRP_{Vh}) is a homodimeric enzyme having a bound FMN per enzyme monomer. The bound FMN functions as a cofactor of FRP_{Vh} in transferring reducing equivalents from NADPH to a flavin substrate in the absence of *V. harveyi* luciferase but as a substrate for FRP_{Vh} in the luciferase-coupled bioluminescent reaction. As part of an integral plan to elucidate the regulation of functional coupling between FRP_{Vh} and luciferase, this study was carried out to characterize the equilibrium bindings, reductive potential, and the reversibility of the reduction of the bound FMN in the reductive half-reaction of FRP_{Vh}. Results indicate that, in addition to NADPH binding, NADP⁺ also bound to FRP_{Vh} in either the oxidized (K_d 180 μ M) or reduced (K_d 230 μ M) form. By titrations with NADP⁺ and NADPH and by an isotope exchange experiment, the reduction of the bound FMN by NADPH was found to be readily reversible ($K_{eq} = 0.8$). Hence, the reduction of FRP_{Vh}-bound FMN is not the committed step in coupling the NADPH oxidation to bioluminescence. To our knowledge, such an aspect of flavin reductase catalysis has only been clearly established for FRP_{Vh}. Although the reductive potentials and some other properties of a R203A variant of FRP_{Vh} and an NADH/NADPH-utilizing flavin reductase from *Vibrio fischeri* are quite similar to that of the wild-type FRP_{Vh}, the reversal of the reduction of bound FMN was not detected for either of these two enzymes.

A growing number of two-component flavin-dependent monooxygenases have been shown to function in a wide scope of biochemical processes such as bacterial bioluminescence (1, 2), biosynthesis of the antibiotic agents valanimycin (3) and actinorhodin (4), and desulfurization of fossil fuel (5). More examples and descriptions of the biochemical properties of selected systems can be found in a recent review (6). Each two-component monooxygenase system consists of a monofunctional monooxygenase and an NAD(P)H-flavin oxidoreductase (or flavin reductase). The former enzyme catalyzes the hydroxylation of a substrate by molecular oxygen utilizing reduced flavin as a cosubstrate. The required reduced flavin is provided by the corresponding flavin reductase, which catalyzes the reduction of flavin at the expense of NAD(P)H.

Because free reduced flavin is subject to autoxidation (7–9), it is intriguing how the various monofunctional monooxygenases efficiently acquire their necessary reduced flavin substrate from the flavin reductases. However, mechanisms of reduced flavin transfer from donor to acceptor enzymes, in two-component monooxygenases or any other reduced flavin-requiring systems, have long evaded elucidation. Only recently, a few selected two-component monooxy-

genases have been subjected to mechanistic investigations with respect to reduced flavin transfer (4, 10, 11). Among them, the bacterial luciferase–flavin reductase system has been studied considerably more extensively.

Bacterial luciferase catalyzes a reaction in which FMNH₂¹ and a long-chain aldehyde are oxidized by molecular oxygen to generate FMN, carboxylic acid, water, and bioluminescence. The required FMNH₂ is provided in vivo by flavin reductases, of which the *Vibrio harveyi* NADPH-preferring flavin reductase P (FRP_{Vh}) (10, 12–18) and the *Vibrio fischeri* NADH/NADPH-utilizing general flavin reductase G (FRG_{Vf}) (10, 16, 19–23) have been characterized in considerable detail. Both FRP_{Vh} and FRG_{Vf} are homodimeric flavoenzymes containing a bound FMN per enzyme monomer. Their crystal structures have been determined (14, 15, 22). Both FRP_{Vh} and FRG_{Vf} undergo a monomer–dimer equilibrium (13, 23). In the case of FRP_{Vh}, the monomeric form is the dominant species in vivo and only the monomer binds to luciferase to form a functional complex (17, 24).

The bound FMN in FRP_{Vh} and FRG_{Vf} holoenzymes has dual functionalities. In the absence of bacterial luciferase, the bound FMN functions as a genuine cofactor, and both reductases follow a ping-pong mechanism (10, 19), which involves the sequential events of NAD(P)H binding, reduction of FMN cofactor, NAD(P)⁺ release, binding and subsequent reduction of a flavin substrate by the reduced

[†] Supported by Grant GM25953 from the National Institutes of Health and Grant E-1030 from The Robert A. Welch Foundation.

* Corresponding author: telephone, 713-743-8359; fax, 713-743-8351; e-mail, dtu@uh.edu.

[‡] Current address: Department of Veterinary Molecular Biology, Montana State University, Bozeman, MT 59717.

[§] Current address: FM:Systems Inc., Raleigh, NC 27609.

^{||} Current address: Church & Dwight, Inc., 326 Half Acre Road, Cranbury, NJ 08512.

¹ Abbreviations: FRP_{Vh} and L_{Vh}, NADPH-preferring flavin reductase P and luciferase, respectively, from *Vibrio harveyi*; FRG_{Vf} and L_{Vf}, NADH/NADPH-utilizing general flavin reductase G and luciferase, respectively, from *Vibrio fischeri*; FMNH₂, reduced riboflavin 5'-phosphate.

cofactor, and, finally, release of the reduced flavin product and regeneration of the original oxidized holoenzyme. The originally bound FMN shuttles between an oxidized and a reduced state but remains bound as a cofactor throughout the catalytic cycle. However, in the presence of their respective luciferase partners, the bound FMN is used by FRP_{Vh} and FRG_{Vf} as a substrate reducible by the NAD(P)H cosubstrate. Both reductases follow a sequential mechanism in generating the reduced flavin product, which is directly transferred to luciferase for the coupled bioluminescence reaction (10, 16), leaving the reductase in an apoenzyme form. The binding of FMN, released from luciferase after the luminescence reaction or made available by other processes, regenerates the FRP_{Vh} and FRG_{Vf} holoenzymes. Moreover, FRP_{Vh} and FRG_{Vf} behave differently in hybrid reductase–luciferase systems (10, 16). FRP_{Vh} follows the same sequential mechanism in reducing and transferring the bound FMN when it is coupled to either the *V. harveyi* luciferase (L_{Vh}) or the *V. fischeri* luciferase (L_{Vf}). In contrast, the coupled reaction of FRG_{Vf} and *V. harveyi* luciferase (L_{Vh}) follows the ping-pong mechanism with the originally bound FMN in the FRG_{Vf} holoenzyme maintaining its functional role as a cofactor. Hence, the mechanism of FMNH₂ transfer between flavin reductase and luciferase appears to be rather delicately regulated by both the reduced flavin donor and acceptor enzymes.

Both FRP_{Vh} and FRG_{Vf} are highly efficient enzymes with turnover rates about 2–3 orders of magnitude faster than their respective luciferase partners. Moreover, the biosynthesis of neither flavin reductase is in concert with the rapid induction of luciferase encoded in the *lux* operon (1, 25, 26). NAD(P)H is a precious energy source for many biochemical and physiological functions. If NAD(P)H is committed to rapid and irreversible oxidation by flavin reductases without a well-controlled functional coupling with luciferase, significant amounts of NAD(P)H would be wasted in generating FMNH₂ for nonproductive autooxidation. Therefore, knowledge on flavin reductases with respect to equilibrium binding of NAD(P)⁺ and NAD(P)H and reversibility of the reduction of bound FMN is essential to an integral understanding of the regulation of NAD(P)H oxidation for bioluminescence. To date, knowledge along these lines is severely limited or lacking for FRP_{Vh} and FRG_{Vf} in particular and for flavin reductases in two-component monooxygenase systems in general. Such a lack of understanding prompted us to carry out this study to elucidate the redox potential and equilibrium properties of the reductive half-reactions of FRP_{Vh} and, to a more limited scope, FRG_{Vf}. We found that, despite many similar properties between FRP_{Vh} and FRG_{Vf} (6), the thermodynamic characteristics of their reductive half-reactions have significant differences. These findings, once again, highlight the delicacy in the functional coupling between specific species of flavin reductase and luciferase.

EXPERIMENTAL PROCEDURES

Materials. NADPH, NADP⁺, NAD⁺, NADH, FMN, benzyl viologen, phenosafranin, NAD⁺ kinase (from liver, type IV), and isocitrate dehydrogenase were all from Sigma. [4-³H]NAD⁺ was obtained from Amersham Biosciences. *V. harveyi* FRP_{Vh} and *V. fischeri* FRG_{Vf} were purified to apparent homogeneity as described previously from *Escherichia coli* harboring pFRP1 (12) and pFRG (10), respectively.

The published methods (18) were followed for the construction and purification of the R203A variant of FRP_{Vh}, in which the arginine residue of the wild-type enzyme at the 203 position was replaced by an alanine residue. Purity of enzyme samples was judged on the basis of sodium dodecyl sulfate–polyacrylamide gel electrophoresis. All phosphate (P_i) buffers were, except noted otherwise, at pH 7.0 and consisted of phosphates at mole fractions of 0.39 sodium monobase and 0.61 potassium dibase.

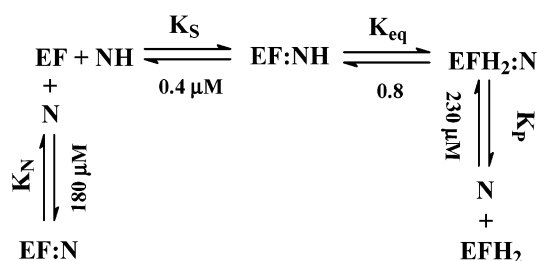
NADPH and NADP⁺ Titrations. One milliliter of the FRP_{Vh} sample in an airtight anaerobic titration cuvette (27) was deoxygenated by three cycles of vacuum application and refilling with N₂. The enzyme sample under N₂ gas was titrated with NADPH and NADP⁺ by using a microsyringe for the addition of small-volume aliquots of concentrated NADPH and/or NADP⁺ stock solutions stepwise through the side arm of the cuvette, and the absorption spectrum of the sample at equilibrium was taken after each addition using a Milton Roy 3000 spectrophotometer. When enzyme was titrated with NADP⁺ in the absence of NADPH, titrations were carried out under aerobic conditions.

Determination of Reductive Potentials. Reductive potentials were determined by dithionite titrations performed using an anaerobic titration cuvette in the same way as described above for NADPH titrations. Aliquots of dithionite at appropriate concentrations in the microsyringe were added stepwise into 1 mL of N₂-saturated solution containing 2 μM benzyl viologen and equal molar concentrations of FRP_{Vh} and phenosafranin. Phenosafranin and benzyl viologen were used as an internal standard and a mediator in electron transfer, respectively. The absorption spectrum at equilibrium was taken after each addition, and spectral data were analyzed according to the Nernst equation.

Synthesis and Purification of [4-³H]NADP⁺. In 10 mL of 70 mM phosphate buffer, pH 7.5, containing 5 mM ATP, 5 mM MgCl₂, 0.2 mM NAD⁺, and 250 μCi of [4-³H]NAD⁺ (cpm 99300 for a 4 μL aliquot) 50 units of NAD⁺ kinase was added (one unit is defined as the phosphorylation of 1 nmol of NAD⁺ to NADP⁺ per minute at pH 7.5 and 37 °C). The solution was incubated for 8 h at room temperature, heated in boiling water for 40 s, cooled on ice, and then loaded onto a DEAE-cellulose column (2 × 22 cm, pre-equilibrated with 70 mM P_i, pH 7.5). The column was washed first with 20 mL of 120 mM P_i, pH 7.5, and then with a linear gradient (300 mL total) from 140 to 240 mM P_i (pH 7.5). Fractions were counted, and those containing [4-³H]NADP⁺ were pooled. The yield was about 14%, with a specific radioactivity of 55 μCi/μmol.

Test for Conversion of [4-³H]NADP⁺ to [4-³H]NADPH by FRP_{Vh}. FRP_{Vh} (0.12 μg) was added to 0.5 mL of P_i, pH 7.0, containing 2 mM NADPH and 0.054 μCi of [4-³H]-NADP⁺ (specific radioactivity 55 μCi/μmol). The solution was incubated at room temperature for 1 h. NADP⁺ (10 mM in 0.01 mL of P_i, pH 7.0, used as a marker for spectrophotometric detection at 260 nm) was added and the mixture was loaded onto a DE-52 column (0.5 × 5 cm, pre-equilibrated with water). The column was sequentially eluted with 1.5 mL of H₂O, 5.5 mL of 85 mM P_i, pH 7.5, and 300 mM P_i, pH 7.5. Fractions were collected at 1 mL each and were counted for radioactivity. A control was run under identical conditions except in the absence of FRP_{Vh}.

Scheme 1



RESULTS

Equilibrium Scheme in the Reductive Half-Reaction. Initial experiments showed that the addition of excess NADPH into FRP_{Vh} only partially bleached the absorbance of its bound FMN in the absence of O₂ and exogenous FMN. Furthermore, the bleaching was partially reversed by the addition of NADP⁺. These findings led us to propose Scheme 1 to account for the reaction steps involved in the reductive half-reaction of FRP_{Vh}. Values of various constants are based on determinations made in this study.

Following this scheme, NADPH (NH) binds to oxidized FRP_{Vh} holoenzyme (EF) to form an EF:NH complex. The bound FMN (F) is reduced by NH in EF:NH to generate the reduced enzyme (EFH₂) which remains in complex with NADP⁺ (EFH₂:N). The release of NADP⁺ (N) from EFH₂:N yields the free reduced enzyme (EFH₂). NADP⁺ is also a competitive inhibitor against NADPH binding. K_N , K_S , and K_P are the dissociation constants for complexes EF:N, EF:NH, and EFH₂:N, respectively, and the equilibrium constant of the conversion of EF:NH to EFH₂:N is defined as $K_{eq} = [\text{EFH}_2\text{:N}]/[\text{EF:NH}]$. This scheme was then subjected to experimental tests as described below.

Aerobic NADP⁺ Titration. Oxidized FRP_{Vh} holoenzyme EF was found capable of binding NADP⁺, resulting in substantial changes in its absorption spectrum. When FRP_{Vh} was titrated with NADP⁺ from 0.1 to 0.98 mM, the difference spectra of (FRP_{Vh} + NADP⁺) – FRP_{Vh} showed two peaks at 392 and 506 nm, two partially overlapped troughs between these two peaks, and two well-defined isosbestic points at 405 and 467 nm (Figure 1A). Changes of ΔA_{506} signals were analyzed according to eq 1 following the method of Wu and Hammes (28)

$$K_N = \frac{[(\text{EF})_0 - P][(\text{N})_0 - nP]}{P} \quad (1)$$

where n and K_N are the number of NADP⁺ binding sites per FRP_{Vh} monomer and the dissociation constant for EF:N, respectively; $(\text{EF})_0$ and $(\text{N})_0$ are the total molar concentrations of oxidized FRP_{Vh} and NADP⁺, respectively; and P is the equilibrium concentration of EF:N. The term P at different $(\text{N})_0$ was calculated using the equation $P = (\Delta A/\Delta A_{\text{max}}) \times (\text{EF})_0$. ΔA_{max} was ΔA_{506} when FRP is saturated with N and was determined to be 0.149 by double reciprocal plotting of ΔA_{506} and $[\text{NADP}^+]$. Equation 1 can be rearranged to eq 2

$$\frac{(\text{N})_0}{P} = \frac{K_N}{(\text{EF})_0 - P} + n \quad (2)$$

(28). Consistent with eq 2, a linear relationship was obtained in plotting $(\text{N})_0/P$ against $1/[(\text{E})_0 - P]$ (Figure 1B). On the

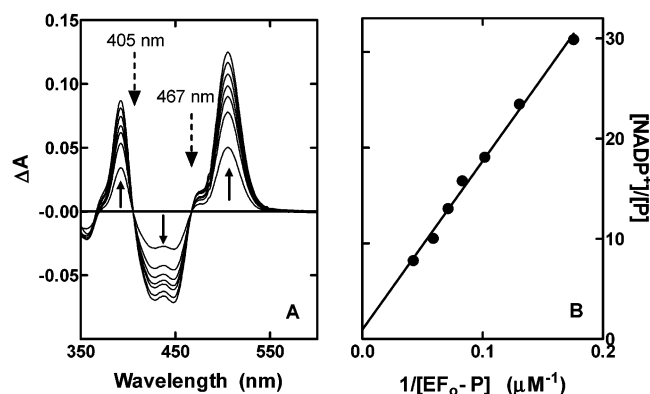


FIGURE 1: Titration of FRP_{Vh} with NADP⁺. (A) A 1 mL solution containing 46 μM FRP_{Vh} in 50 mM P_i was titrated with NADP⁺ (at total NADP⁺ concentrations of 0.1, 0.2, 0.3, 0.39, 0.49, 0.69, and 0.98 mM) at 23 °C. The spectrum of the sample was recorded before NADP⁺ addition and when the binding reached equilibrium after each addition. The difference spectra (FRP_{Vh} + NADP⁺) – FRP_{Vh} are presented as a function of NADP⁺ concentration with the solid line arrows indicating the direction of absorbance change with increasing amounts of NADP⁺. Two well-defined isosbestic points (shown as ΔA = 0) are indicated by the dashed arrows. (B) ΔA_{506} was analyzed according to eq 2, allowing the calculation of the dissociation constant and number of NADP⁺ binding sites from the slope and intercept, respectively.

basis of values of the intercept on the ordinate and the slope, FRP_{Vh} was found to bind 0.99 NADP⁺ per enzyme monomer with $K_N = 1.8 \times 10^{-4}$ M.

Anaerobic NADP⁺ Titration. In the presence of saturating NADPH, [EF] and [EF:N] in Scheme 1 are negligible. Therefore, eq 3 describes the relationship between [N] and

$$\frac{[\text{E}_{\text{red}}]}{[\text{E}_{\text{ox}}]} = \frac{[\text{EFH}_2\text{:N}] + [\text{EFH}_2]}{[\text{EF:NH}]} = K_{eq} + \frac{K_{eq}K_P}{[\text{N}]} \quad (3)$$

the ratio of total reduced FRP_{Vh} over total oxidized FRP, i.e., $[\text{E}_{\text{red}}]/[\text{E}_{\text{ox}}]$, at equilibrium. To test eq 3, FRP_{Vh} was titrated with NADP⁺ in the presence of a high concentration of NADPH, and the spectrum was recorded before and after the addition of NADPH and each addition of NADP⁺. The absorption peak of the oxidized FRP_{Vh} at 453 nm was bleached by about 87% upon the reduction of FRP_{Vh} by saturating NADPH without any addition of NADP⁺. The bleaching was gradually but partially reversed when increasing levels of NADP⁺ were added (Figure 2A). When increases in A_{453} were plotted as a function of the NADP⁺ concentration, a hyperbolic curve was obtained reaching about 55% of the original A_{453} before bleaching by NADPH (not shown). Such absorbance increases due to the NADP⁺ additions were not reversed by further addition of NADPH, indicating that NADPH was indeed saturating. In principle, the EF species would partition between EF:NH and EF:N in the presence of NADPH and NADP⁺. A complete recovery of the oxidized FRP_{Vh} should occur when a sufficiently high level of NADP⁺ was added to out-compete NADPH in this partitioning. However, additions of NADP⁺ only led to a partial recovery of the oxidized reductase (Figure 2A). This is because the level of NADPH originally added (0.3 mM) was 750-fold of the K_S whereas the highest level of NADP⁺ added (2.1 mM) was only 11.7-fold of K_N . Hence the partitioning between EF:NH and EF:N strongly favors the former under our experimental conditions. There-

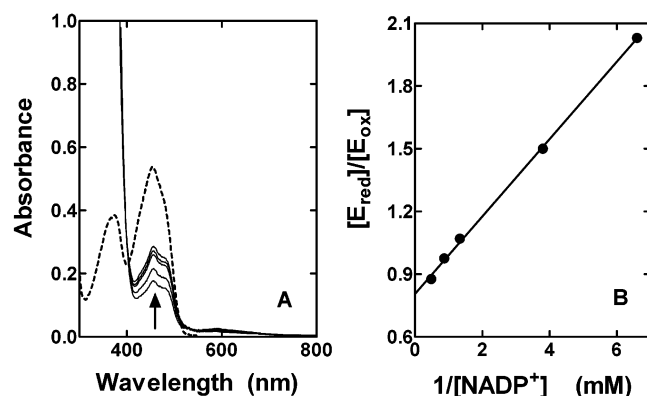


FIGURE 2: Anaerobic titration of FRP_{vh} with NADP⁺ in the presence of NADPH. (A) FRP_{vh}, at 40 μM, in 1 mL of N₂-saturated 50 mM P_i containing 0.3 mM NADPH was titrated anaerobically at 23 °C with 0.15–2.1 mM NADP⁺. Spectra were taken after stepwise titrations when equilibria were achieved. The arrow shows the direction of spectrum change with increasing amount of NADP⁺. The spectrum of FRP_{vh} without NADPH or NADP⁺ is also presented (dashed line) as a reference. (B) [E_{red}]/[E_{ox}], concentration ratio of total reduced over total oxidized FRP_{vh}, is plotted against the reciprocal of [NADP⁺] using the data from panel A.

fore, the partial recoveries of oxidized FRP_{vh} upon NADP⁺ additions were primarily a consequence of the reversion of EFH₂ to EFH₂:N and the subsequent equilibrium between EFH₂:N and EF:NH.

It should be noted that low levels of absorption in the 540–700 nm range were detectable after NADP⁺ addition (Figure 2A). Species contributing to such absorption could be flavin semiquinone (29) or the charge complex of EF:NH and/or EFH₂:N, similar to those observed for *E. coli* flavin reductase Fre (30). However, the amounts of long-wavelength-absorbing species were quite low. Hence, for simplicity, these species are not included in Scheme 1. Accordingly, absorbance signals at 453 nm (Figure 2A) provide a measure of the total oxidized enzyme (*E*_{ox}) and total reduced enzyme (*E*_{red} = *E*_{total} – *E*_{ox}). The total NADP⁺ concentration was determined from the level of added NADP⁺ and the amount of NADPH oxidation. Data shown in Figure 2A can then be analyzed according to eq 3 as shown in Figure 2B. As expected, a linear relationship was observed between the ratio of [E_{red}]/[E_{ox}] and the reciprocal of NADP⁺ concentration. On the basis of the intercept on the ordinate and the slope, *K*_{eq} and *K*_P were determined to be 0.8 and 2.3 × 10^{−4} M, respectively.

The possible formation of an EFH₂:NH complex between NADPH and reduced enzyme E:FH₂ was considered. However, the recovery of oxidized flavin absorbance upon the addition of NADP⁺ was not reversed by further addition of NADPH (Figure 2A), suggesting that the EFH₂:NH complex formation was negligible in competition with the EFH₂:N formation under our experimental conditions. Hence, EFH₂:NH is not included in Scheme 1.

NADPH Titration. The spectra were measured under anaerobic conditions after each addition of a small aliquot of NADPH into N₂-saturated FRP_{vh} containing a constant level of 3 mM NADP⁺. Higher levels of FRP_{vh} reduction (indicated by decreasing *A*₄₅₀) were observed at increasing levels of NADPH addition (Figure 3A). Since the NADP⁺ level was 13 times the *K*_P, free fully reduced FRP_{vh} (EFH₂)

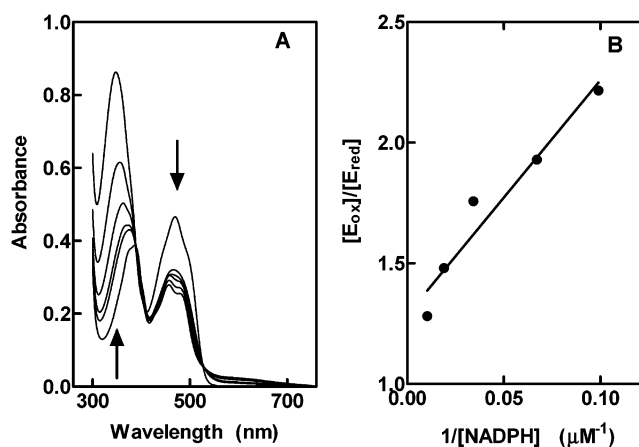


FIGURE 3: Anaerobic titration of FRP_{vh} with NADPH in the presence of NADP⁺. (A) Absorption spectra of FRP_{vh} after stepwise addition of NADPH into 1 mL of N₂-saturated P_i containing 40 μM FRP_{vh} and 3 mM NADP⁺ at 23 °C under anaerobic conditions. The total concentrations of NADPH immediately after addition were, in the direction of arrows, 0, 60, 80, 100, 140, and 200 μM. (B) Plots of [E_{ox}]/[E_{red}] versus the reciprocal of free NADPH concentration using data derived from panel A.

should not exist in any significant amounts. Therefore, the data in Figure 3A can be analyzed according to eq 4 derived

$$\frac{[E_{ox}]}{[E_{red}]} = \frac{[EF] + [EF:N] + [EF:NH]}{[EFH_2:N]} = \frac{1}{K_{eq}} + \frac{K_S(K_N + [N])}{K_N K_{eq} [NH]} \quad (4)$$

from Scheme 1. The absorbance at 467 nm, an isosbestic point in the conversion between EF and EF:N (Figure 1A), was used to calculate the total amount of the oxidized FRP_{vh} species assuming that EF:NH has a similar absorptivity at this wavelength. Free NADPH concentrations were determined from the observed *A*₃₄₀ after corrections for *A*₃₄₀ contributed by FRP_{vh} and the enzyme-bound NADPH. The concentration of bound NADPH was determined from the relationship [EF:NH] = [EFH₂:N]/*K*_{eq} = [E_{red}]/*K*_{eq}. As predicted by eq 4, [E_{ox}]/[E_{red}] versus 1/[NADPH] showed a linear line (Figure 3B), allowing the determination of *K*_{eq} = 0.8 and, based on *K*_N determined from Figure 1, *K*_S = 0.4 μM. The value of *K*_{eq} determined from this NADPH titration correlated well with that determined from the anaerobic NADP⁺ titration shown in Figure 2.

Reductive Potential. The reductive potential of FRP_{vh} was determined by spectral titration with dithionite using the phenosafranin redox couple as a standard. The absorption peaks of oxidized FRP_{vh} and phenosafranin (PS) at 453 and 520 nm, respectively, can be completely bleached upon full reduction by dithionite. After the addition of a given amount of dithionite, an equilibrium state was reached for both redox pairs of FRP_{vh,ox}/FRP_{vh,red} and PS_{ox}/PS_{red}. Spectral measurements of the sample at various equilibrium states after the addition of increasing amounts of dithionite are shown in Figure 4A. At each equilibrium state, the concentration ratio of oxidized over reduced phenosafranin ([PS_{ox}]/[PS_{red}]) was determined from the ratio of *A*₅₄₀/Δ*A*₅₄₀, where *A*₅₄₀ is the observed absorbance at equilibrium state and Δ*A*₅₄₀ is the original absorbance minus *A*₅₄₀. FRP_{vh} had no contribution

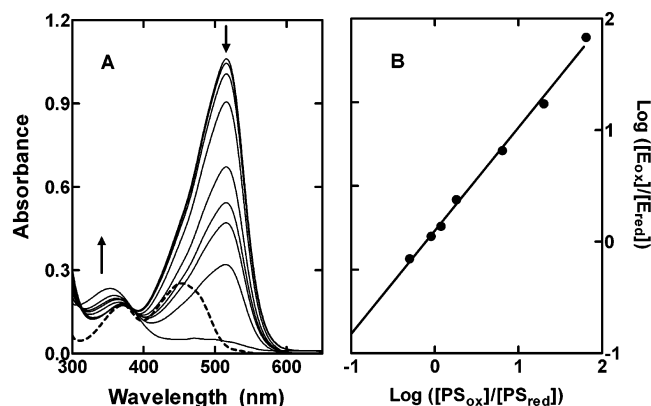


FIGURE 4: Determination of the reductive potential of FRP_{vh}. Aliquots of dithionite were added into 1 mL of 50 mM P_i containing 20 μ M phenosafranin, 2 μ M benzyl viologen, and 20 μ M FRP_{vh}. (A) Changes of the sample spectra with increasing amounts of dithionite addition are shown in the direction of the arrows. The spectrum of FRP_{vh} before dithionite addition is shown as the dashed line. (B) At each equilibrium state after the addition of dithionite, the ratio of oxidized over reduced phenosafranin ($[PS_{ox}]/[PS_{red}]$) was determined from the ratio of $A_{540}/\Delta A_{540}$, where A_{540} is the observed absorbance at equilibrium state and ΔA_{540} is the original absorbance minus A_{540} . The ratio of oxidized over reduced FRP_{vh} ($[E_{ox}]/[E_{red}]$) was similarly determined from $A_{465}/\Delta A_{465}$, where all absorbance readings at 465 nm were corrected for the contributions from oxidized phenosafranin. The log–log plot of $[E_{ox}]/[E_{red}]$ versus $[PS_{ox}]/[PS_{red}]$ is presented.

to observed A_{540} . The concentration ratio of oxidized over reduced FRP_{vh} ($[E_{ox}]/[E_{red}]$) was similarly determined from $A_{465}/\Delta A_{465}$ where all absorbance readings at 465 nm were corrected for the contributions from oxidized phenosafranin. These data can be analyzed following the rearranged Nernst equation:

$$\log([E_{ox}]/[E_{red}]) = (\Delta E^{\circ}_{PS} - \Delta E^{\circ}_{FRP}) \frac{2F}{2.303RT} + \log([PS_{ox}]/[PS_{red}]) \quad (5)$$

The log–log plot of $[E_{ox}]/[E_{red}]$ against $[PS_{ox}]/[PS_{red}]$ using data from Figure 4A gives a linear line (Figure 4B) with a slope of 0.95 and an intercept of 0.098. Accordingly, the standard reductive potential of FRP_{vh} was calculated to be -255 mV using the intercept and -252 mV for ΔE°_{PS} .

For an accurate determination of the standard reductive potential of FRP_{vh} by the method summarized above, there should be no significant binding of phenosafranin by FRP_{vh} so that the known ΔE°_{PS} of -252 mV for free phenosafranin can be applied to eq 5. This critical requirement was confirmed by equilibrium dialysis measurements. FRP_{vh} (0.5 mL, 55 μ M) was put into a Slide-A-Lyzer cassette with 10000 MWCO (Pierce) and dialyzed against 500 mL of 100 μ M phenosafranin in 50 mM P_i for 24 h. The phenosafranin level in the FRP_{vh}-containing sample was spectrally determined to be 101 μ M in comparison with 100 μ M in the outside solution. Apparently FRP_{vh} did not bind phenosafranin significantly under our experimental conditions.

Reduction of FRP_{vh} R203A. FRP_{vh} R203A has very low affinities for both NADPH and NADP⁺ but is catalytically active (18). As shown in Figure 5, R203A was completely reduced by NADPH in the presence of 0.26 mM NADP⁺ under anaerobic conditions. This is in sharp contrast with wild-type FRP_{vh} that had about 50% in oxidized form under

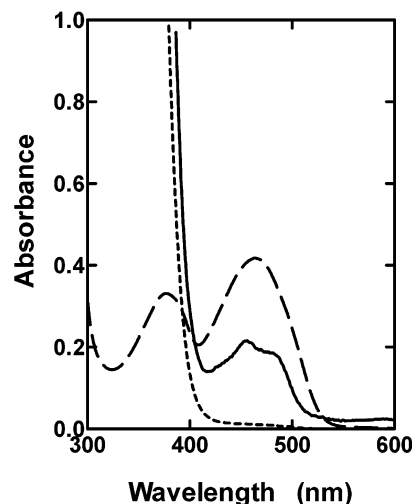


FIGURE 5: Comparison of wild-type and the R203A variant of FRP_{vh} in their reduction by NADPH in the presence of NADP⁺. Spectra of 40 μ M wild-type (solid line) and R203A (short dashed line) FRP_{vh} were taken under anaerobic conditions in the presence of 0.3 mM NADPH and 0.26 mM NADP⁺. The off-scale absorbance in the region of <400 nm was mainly from NADPH, and the bleaching of the A_{450} peak was due to the reduction of FRP_{vh} enzymes. The spectrum of R203A (long dashed line) before the addition of NADP⁺ and NADPH is also presented as a reference.

the same conditions. The reductive potential of FRP_{vh} R203A was previously determined to be -259 mV (18).

NAD⁺ Binding by and Reductive Potential of FRG_{vf}. Addition of NAD⁺ up to 10 mM did not change the spectrum of FRG_{vf}. FRG_{vf} remained in a completely reduced state in the presence of 0.3 mM NADH and NAD⁺ at levels up to 10 mM under anaerobic condition. The reductive potential of FRG_{vf} was determined to be -215 mV by the dithionite titration similar to that described above for FRP_{vh}.

Reversibility of FRP Reduction by NADPH. When FRP_{vh} was mixed with NADPH and $[4\text{-}^3\text{H}]\text{NADP}^+$ without any exogenously added FMN, the enzyme can only carry out the first half of the overall reaction to allow the reduction of bound FMN and the production of NADP⁺. If the conversion of EF:NH to EFH₂:N (Scheme 1) is irreversible, there should be no reduction of NADP⁺ back to NADPH. However, as shown in Figure 6, the labeled $[4\text{-}^3\text{H}]\text{NADP}^+$ in the solution was significantly converted to NADPH in the presence of FRP_{vh}. Clearly, the step of FRP_{vh} holo-enzyme reduction by NADPH is readily reversible.

DISCUSSION

Although FRP_{vh} and FRG_{vf} share a number of similarities with respect to their mechanistic and structural properties (6), there are significant differences between these two reductases as well. FRP_{vh} strongly prefers NADPH as a substrate and has a disordered loop within which the Arg203 residue is critical to NADPH recognition and binding (18). On the other hand, FRG_{vh} does not have this disordered loop and can utilize NADH and NADPH with similar efficiencies. Moreover, in hybrid-coupled reactions of FRP_{vh}–L_{vf} and FRG_{vf}–L_{vh}, the two reductases follow different mechanisms in reducing their originally bound FMN (10, 16). In this study, the binding of reduced and oxidized pyridine nucleotides and the redox properties have been characterized for FRP_{vh} and, for some critical comparisons, also for a R203A

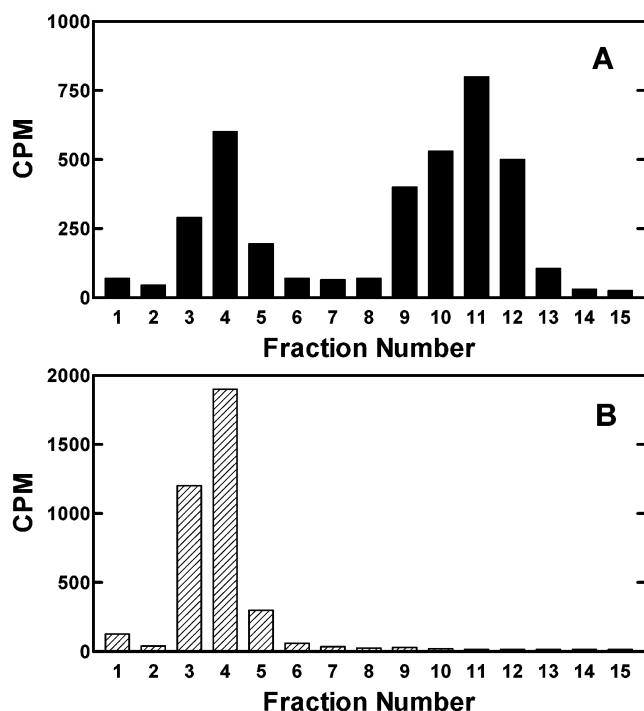


FIGURE 6: Reversibility of FRP_{vh} reduction by NADPH. (A) A reaction solution containing 0.12 μg of FRP_{vh}, 2 mM NADPH, and 0.054 μCi of [4-³H]NADP⁺ (specific radioactivity = 55 $\mu\text{Ci}/\mu\text{mol}$) in 0.5 mL of 50 mM P_i, pH 7.5, was incubated for 1 h. Unlabeled NADP⁺ (0.01 mL of a 10 mM stock) was then added as a marker. The solution was subjected to chromatography on a DE-52 column as described in the text, and 1 mL fractions were collected and counted for tritium. (B) A control run under conditions identical to that described for panel A except without any addition of FRP_{vh}. The peak (at fraction 4) in both panels is associated with NADP⁺ whereas the second peak (at fraction 11) in panel A is associated with NADPH based on another control run using NADPH only.

variant of FRP_{vh} and for FRG_{vf}. Again, some significant differences were uncovered.

We have shown that monomeric FRP_{vh} can form a complex with luciferase that is functionally active in vitro and in vivo (17, 24). This satisfies a critical requirement for a direct metabolite channeling system. However, FRP_{vh} is constitutively synthesized (26) whereas the biosynthesis of L_{vh} is subjected to the induction of the *lux* operon (1). During the life cycle of *V. harveyi*, periods must exist in which part or even most of the FRP_{vh} molecules are not functionally coupled to luciferase. Moreover, FRP_{vh} has a k_{cat} of 4170 min^{-1} (18), much faster than the 2–20 min^{-1} k_{cat} (depending upon the aldehyde substrate) for luciferase (31). If FRP_{vh} is allowed to rapidly and irreversibly convert NADPH to NADP⁺ for the formation of nonproductive FMNH₂, not only precious NADPH would be wasted but also toxic oxygen species would be generated from autoxidation of reduced flavin. This study demonstrated for the first time that, in addition to forming a structural and functional complex with luciferase (17, 24), the utilization of NADPH by FRP_{vh} is sensitive to other factors for regulation.

First and foremost, the step of reduction of the bound FMN is readily reversible as indicated by the finding of $K_{\text{eq}} = [\text{EFH}_2\text{N}]/[\text{EF:NH}] = 0.8$ on the basis of results of NADP⁺ titration in the presence of saturating NADPH (Figure 2) and NADPH titration in the presence of saturating NADP⁺ (Figure 3). In another independent test, [4-³H]NADP⁺ was

found to be converted back to [4-³H]NADPH in the reductive half-reaction of FRP_{vh} (Figure 6). Therefore, the reversibility of reduction of the bound FMN by NADPH has been clearly established for FRP_{vh}. The physiological implication of this finding is that the reduction of the bound FMN of FRP_{vh} by NADPH is not the committed step in NADPH oxidation. It should be noted that, whenever FRP_{vh} is not completely trapped by L_{vh} in complex formation, the reversibility of the reduction of FRP_{vh}-bound FMN would decrease but not prevent the formation of reduced flavin that is uncoupled from luciferase bioluminescence. The reduced flavin so generated by FRP_{vh} would be a wasteful product if the sole function of FRP_{vh} in vivo is to provide FMNH₂ for luciferase. However, in metabolite channeling, a completely leak-free coupling of a donor enzyme with one acceptor enzyme may not be desirable if the metabolite generated by the former is needed by other enzymes or processes. In this connection, the possibility remains that the reduced flavin generated by FRP_{vh} may have other acceptor enzymes. There is yet another level of regulation shared by FRP_{vh} and FRG_{vf} to reduce wasteful oxidation of NAD(P)H. The $K_{\text{m,NADPH}}$ of FRP_{vh} and the $K_{\text{m,NADH}}$ of FRG_{vf} are 0.02 and 9 μM , respectively, when coupled to luciferase but are markedly elevated to 20 and 120 μM , respectively, when free from coupling with luciferase (10). This would decrease the abilities of both reductases, when they are not functionally coupled to luciferase, to compete with other NAD(P)H utilizing enzymes in the cells.

The reversibility of reduction of the reductase-bound FMN is quite sensitive to perturbation. When R203A is compared with the wild-type FRP_{vh}, this mutation results in a marked elevation of K_{m} for NADPH but only small changes in its standard reductive potential, K_{d} for FMN cofactor binding, K_{m} for flavin substrate, and k_{cat} (18). However, in sharp contrast to wild-type FRP_{vh}, R203A was fully reduced by NADPH in the presence of 0.26 mM NADP⁺ (Figure 5), showing no detectable degree of reversal of the reduction of FMN cofactor. FRG_{vf} also has a standard reductive potential similar to that of FRP_{vh}. However, different from FRP_{vh}, full reduction of FRG_{vf} was obtained at 0.3 mM NADH, and no reversal of the reduction of the bound FMN was observed by the addition of NAD⁺ up to 10 mM. The reversibility of FRP_{vh} in NADPH oxidation is further in contrast to the irreversibility of reduction of flavin substrate by NADPH catalyzed by the *E. coli* flavin reductase Fre, which does not utilize flavin as a cofactor and follows a sequential mechanism (30). To date, the particular aspect of reversibility of flavin reduction/NAD(P)H oxidation has, to our knowledge, only been demonstrated for FRP_{vh}.

In addition to NADPH binding, NADP⁺ also binds to oxidized and reduced FRP_{vh} with dissociation constants of 180 μM (Figure 1) and 230 μM (Figure 2), respectively. As shown in Scheme 1, the NADP⁺ binding to EFH₂ would favor the reversal of NADP⁺ to NADPH, and NADP⁺ binding to EF would trap FRP_{vh} in a form inactive in oxidizing NADPH. Qualitatively, these properties of FRP_{vh} allow another level of regulation of NADPH oxidation by this reductase. Because no information is available on the NADP⁺ level at different stages of the life cycle of luminous bacteria, the physiological significance of such a regulation is uncertain at the present.

REFERENCES

1. Hastings, J. W., Potrikus, C. J., Gupta, S. C., Kurfürst, M., and Makemson, J. C. (1985) Biochemistry and physiology of bioluminescent bacteria, *Adv. Microb. Physiol.* 26, 235–291.
2. Tu, S.-C. (2003) Bacterial Bioluminescence: Biochemistry, in *CRC Handbook of Organic Photochemistry and Photobiology* (Horspool, W. M., and Lenci, F., Eds.) pp 136.1–136.17, CRC Press, Boca Raton, FL.
3. Parry, R. J., and Li, W. (1997) Purification and characterization of isobutylamine N-hydroxylase from the valanimycin producer *Streptomyces viridifaciens* MG456-hF10, *Arch. Biochem. Biophys.* 339, 47–54.
4. Valton, J., Filisetti, L., Fontecave, M., and Nivière, V. (2004) A two-component flavin-dependent monooxygenase involved in actinorhodin biosynthesis in *Streptomyces coelicolor*, *J. Biol. Chem.* 279, 44362–44369.
5. Lei, B., and Tu, S.-C. (1996) Gene overexpression, purification, and identification of a desulfurization enzyme from *Rhodococcus* sp. strain IGTS8 as a sulfide/sulfoxide monooxygenase, *J. Bacteriol.* 178, 5699–5705.
6. Tu, S.-C. (2001) Reduced flavin: Donor and acceptor enzymes and mechanisms of channeling, *Antioxid. Redox Signaling* 3, 881–897.
7. Gibson, Q. H., and Hastings, J. W. (1962) The oxidation of reduced flavin mononucleotide by molecular oxygen, *Biochem. J.* 83, 368–377.
8. Massey, V., Palmer, G., and Ballou, D. (1973) On the reaction of reduced flavins with molecular oxygen, in *Oxidases and Related Redox Systems* (King, J. E., Mason, H. S., and Morrison, M., Eds.) Vol. 1, pp 25–43, University Park Press, Baltimore, MD.
9. Eberlein, G., and Bruice, T. C. (1983) The chemistry of a 1,5-diblocked flavin. 2. Proton and electron-transfer steps in the reaction of dihydroflavins with oxygen, *J. Am. Chem. Soc.* 105, 6685–6697.
10. Lei, B., and Tu, S.-C. (1998) Mechanism of reduced flavin transfer from *Vibrio harveyi* NADPH–FMN oxidoreductase to luciferase, *Biochemistry* 37, 14623–14629.
11. Louie, T. M., Xie, X. S., and Xun, L. (2003) Coordinated production and utilization of FADH₂ by NAD(P)H-flavin oxidoreductase and 4-hydroxyphenylacetate 3-monooxygenase, *Biochemistry* 42, 7509–7517.
12. Lei, B., Liu, M., Huang, S., and Tu, S.-C. (1994) *Vibrio harveyi* NADPH-flavin oxidoreductase: cloning, sequencing and overexpression of the gene and purification and characterization of the cloned enzyme, *J. Bacteriol.* 176, 3552–3558.
13. Liu, M., Lei, B., Ding, Q., Lee, J. C., and Tu, S.-C. (1997) *Vibrio harveyi* NADPH:FMN oxidoreductase: preparation and characterization of the apoenzyme and monomer–dimer equilibrium, *Arch. Biochem. Biophys.* 337, 89–95.
14. Tanner, J. J., Lei, B., Tu, S.-C., and Krause, K. L. (1996) Flavin reductase P: structure of a dimeric enzyme that reduces flavin, *Biochemistry* 35, 13531–13539.
15. Tanner, J. J., Tu, S.-C., Barbour, L. J., Barnes, C. L., and Krause, K. L. (1999) Unusual folded conformation of nicotinamide adenine dinucleotide bound to flavin reductase P, *Protein Sci.* 8, 1725–1732.
16. Jeffers, C. E., and Tu, S.-C. (2001) Differential transfers of reduced flavin cofactor and product by bacterial flavin reductase to luciferase, *Biochemistry* 40, 1749–1754.
17. Jeffers, C. E., Nichols, J. C., and Tu, S.-C. (2003) Complex formation between *Vibrio harveyi* luciferase and monomeric NADPH:FMN oxidoreductase, *Biochemistry* 42, 529–534.
18. Wang, H., Lei, B., and Tu, S.-C. (2000) *Vibrio harveyi* NADPH–FMN oxidoreductase Arg203 as a critical residue for NADPH recognition and binding, *Biochemistry* 39, 7813–7819.
19. Tu, S.-C., Becvar, J. E., and Hastings, J. W. (1979) Kinetic studies on the mechanism of bacterial NAD(P)H:flavin oxidoreductase, *Arch. Biochem. Biophys.* 193, 110–116.
20. Zenno, S., Saigo, K., Kanoh, H., and Inouye, S. (1994) Identification of the gene encoding the major NAD(P)H-flavin oxidoreductase of the bioluminescent bacterium *Vibrio fischeri* ATCC 7744, *J. Bacteriol.* 176, 3536–3543.
21. Inouye, S. (1994) NAD(P)H-flavin oxidoreductase from the bioluminescent bacterium, *Vibrio fischeri* ATCC 7744, is a flavoprotein, *FEBS Lett.* 347, 163–168.
22. Koike, H., Sasaki, H., Kobori, T., Zenno, S., Saigo, K., Murphy, M. E., Adman, E. T., and Tanokura, M. (1998) 1.8 Å crystal structure of the major NAD(P)H:FMN oxidoreductase of a bioluminescent bacterium, *Vibrio fischeri*: overall structure, cofactor and substrate-analog binding, and comparison with related flavoproteins, *J. Mol. Biol.* 280, 259–273.
23. Tang, C. K., Jeffers, C. E., Nichols, J. C., and Tu, S.-C. (2001) Flavin specificity and subunit interaction of *Vibrio fischeri* general NAD(P)H-flavin oxidoreductase FRG/FRase I, *Arch. Biochem. Biophys.* 392, 110–116.
24. Low, J. C., and Tu, S.-C. (2003) Energy transfer evidence for *in vitro* and *in vivo* complexes of *Vibrio harveyi* flavin reductase P and luciferase, *Photochem. Photobiol.* 77, 446–452.
25. Duane, W., and Hastings, J. W. (1975) Flavin mononucleotide reductase of luminous bacteria, *Mol. Cell. Biochem.* 6, 53–64.
26. Jablonski, E., and DeLuca, M. (1978) Studies of the control of luminescence in *Benecke harveyi*: properties of the NADH and NADPH:FMN oxidoreductases, *Biochemistry* 17, 672–678.
27. Williams, C. H., Jr., Arscott, L. D., Matthews, R. G., Thorpe, C., and Wilkinson, K. D. (1979) Methodology employed for anaerobic spectrophotometric titrations and for computer-assisted data analysis, *Methods Enzymol.* 62, 185–198.
28. Wu, C.-W., and Hammes, G. G. (1973) Relaxation spectra of aspartate transcarbamylase. Interaction of the native enzyme with an adenosine 5′-triphosphate analog, *Biochemistry* 12, 1400–1408.
29. Massey, V., and Palmer, G. (1966) On the existence of spectrally distinct classes of flavoprotein semiquinones. A new method for the quantitative production of flavoprotein semiquinones, *Biochemistry* 5, 3181–3189.
30. Nivière, V., Vanoni, M. A., Zanetti, G., and Fontecave, M. (1998) Reaction of NAD(P)H:flavin oxidoreductase from *Escherichia coli* with NADPH and riboflavin: Identification of intermediates, *Biochemistry* 37, 11879–11887.
31. Tu, S.-C. (1979) Isolation and properties of bacterial luciferase-oxygenated flavin intermediate complexed with long-chain alcohols, *Biochemistry* 18, 5940–5945.

BI047952S